

1 **A multidisciplinary approach to estimating red snapper, *Lutjanus campechanus*, behavioral**  
2 **response to mobile camera and sonar sampling gears**

3  
4 Steven B. Garner<sup>a,\*</sup>, Robert Ahrens<sup>a</sup>, Kevin M. Boswell<sup>b</sup>, Matthew D. Campbell<sup>c</sup>, Daniel Correa<sup>b</sup>,  
5 Joseph H. Tarnecki<sup>a</sup>, and William F. Patterson III<sup>a</sup>

6  
7 <sup>a</sup> *University of Florida, Fisheries and Aquatic Sciences, 7922 NW71st St, Gainesville, FL 32653,*  
8 *USA*

9 <sup>b</sup> *Florida International University, Biological Sciences, Biscayne Bay Campus, 3000 NE 151<sup>st</sup> St,*  
10 *North Miami, FL 33181, USA*

11 <sup>c</sup> *National Marine Fisheries Service, Southeast Fisheries Science Center, Mississippi*  
12 *Laboratories, 3209 Frederic St, Pascagoula, MS 39567, USA*

13  
14  
15 \* Corresponding author

16 *E-mail* addresses: sgarner@ufl.edu (SBG)\*

17 kevin.boswell@fiu.edu (KMB)

18 will.patterson@ufl.edu (WFP).

19  
20  
21  
22  
23 **Keywords:** gear bias, acoustic telemetry, ROV, red snapper, Gulf of Mexico

24 We examined the potential for Gulf of Mexico red snapper (RS) behavior to bias count estimates  
25 collected with a remotely operated vehicle (ROV), towed camera sled (TCS), subsurface towed  
26 acoustic sled (TAS), or SCUBA diver at artificial reef sites. Near- ( $\leq 5$  m), mid- ( $\leq 15$  m), and far-  
27 field ( $\leq 100$  m) responses were examined using stationary stereo cameras, a horizontal acoustic  
28 profiler, and three-dimensional acoustic telemetry, respectively. Survey gears were deployed  
29 sequentially for 15 minutes with each gear immediately preceded by a 15-minute control period.  
30 Near-field data (mean RS  $\text{minute}^{-1}$ ) indicated counts were 7.3 times higher with the diver present  
31 and 1.9 times higher with the ROV. The TCS had a significant interaction effect with time on  
32 mean RS count in the near- and mid-field, as well as depth and acceleration. The TAS had no  
33 effect on RS behavior at any scale. Far-field data showed no significant effect of any gear on  
34 mean RS distance to reef. Overall, results indicate RS respond neutrally to survey gears at  
35 medium ( $\leq 15$  m) to large ( $\leq 100$  m) spatial scales, but small-scale ( $\leq 5$  m) spatial attraction may  
36 bias RS counts with benthic survey gears, primarily by individuals near the periphery of the  
37 surveyed area approaching the gear.

## 38 1. Introduction

39

40 Abundance estimates provide important information for single-species or ecosystems-based  
41 assessments of fish populations (Hutchings et al., 2010; Stuart-Smith et al., 2013; Edgar and  
42 Stuart-Smith, 2014; FAO, 2018). Many types of stock assessment models rely on time series of  
43 catch and effort data to estimate total population size, with indices of abundance from both  
44 fishery-dependent and -independent data included when possible to track population trends  
45 (Chen et al., 2003; Haddon, 2010; Hutchings et al., 2010; Maunder and Punt, 2013). Indices of  
46 abundance, while useful, can only track relative interannual changes but are not typically scaled  
47 to total abundance. In contrast, absolute abundance estimates provide an alternative approach to  
48 assessing stock size when density estimates are available for all habitats occupied by the stock,  
49 the sampling window is appropriate for the scale of movement of individuals, and detectability is  
50 well estimated (Fréon, et al. 1993; Rivoirard et al., 2008; Keiter et al., 2017). Rather than  
51 working backwards to estimate stock abundance using landings, demographic, and relative  
52 abundance data via an assessment model, absolute abundances are derived through direct  
53 estimation *in situ*. Expanded direct counts also provide a method to scale time series of relative  
54 indices to an absolute abundance estimate, which then can be used to understand historic stock  
55 size, as well as current stock productivity. Habitat-specific density estimates are scaled up to the  
56 total areal extent of each strata provided that habitat-specific detectability and gear biases are  
57 known and the area surveyed is estimated reliably for each sample (Rivoirard et al., 2008;  
58 Marques et al., 2013; Keiter et al., 2017). The precision of the population estimate is then  
59 dependent upon the sample size relative to the variance of density estimates (Rivoirard et al.,  
60 2008; Ramsey et al., 2015; Keiter et al., 2017).

61 A species inhabiting multiple habitat types likely requires multiple sampling gears, each  
62 with potential biases that must be evaluated in order to provide robust density estimates (Watson  
63 et al., 2005; Schramm et al., 2020). Deploying mobile survey gears allows estimation of the area  
64 swept, with common mobile survey gears including subsurface acoustic profilers (Kotwicki et  
65 al., 2013; Davison et al., 2015), stationary or mobile digital video camera systems (Koslow et al.,  
66 1995; Shortis and Harvey, 1998; Letessier et al., 2015; Schramm et al., 2020), or visual census  
67 techniques with divers (Bohnsack and Bannerot, 1986; Thompson and Mapstone, 1997;  
68 Schramm et al., 2020). Subsurface acoustic profilers are best suited for estimating fish  
69 abundance over large areas in simple habitats with low species-diversity (Lawson and Rose,  
70 1999; Kotwicki et al., 2013; Davison et al., 2015). Stationary camera systems are often effective  
71 in sampling relatively small areas of complex habitat (Somerton and Gledhill, 2005; Watson et  
72 al., 2005; Schramm et al., 2020), while towed cameras or remotely operated vehicles (ROVs) are  
73 effective for sampling either large or small areas of simple or complex habitat depending on the  
74 sled or ROV design (Somerton and Gledhill, 2005; Schramm et al., 2020). Sub-surface acoustic  
75 surveys may lose resolution over complex habitats with diverse fish communities (Lawson and  
76 Rose, 1999; Zenone et al., 2017). Mobile gears (Somerton and Gledhill, 2005; Lorange and  
77 Trenkel, 2006; Stoner et al., 2008; Somerton et al., 2017) or divers (Brock, 1982; Cailliet et al.,  
78 1999; Edgar et al., 2004; Dickens et al., 2011) may elicit positive or negative behavioral  
79 responses. Estimating the area viewed with stationary cameras is often possible, but estimating  
80 fish density (i.e., number per area) can be problematic because it is difficult to determine the  
81 spatial origin of observed fish on video, especially for baited camera rigs, and extended  
82 deployments increase the likelihood of double counting individuals (Harvey et al., 2007;  
83 Langlois et al., 2010; Schramm et al., 2020).

84 Reef fish densities are especially difficult to estimate due to myriad factors influencing the  
85 ability to detect and accurately count within a surveyed area. Reef fish communities are highly  
86 diverse including cryptic and shy species that take cover in crevices while large mobile predators  
87 can easily move beyond the range of visual identification. With optical methods in clear water,  
88 one can assume that relatively large, non-cryptic species are fully detectable within the sampled  
89 area (MacNeil et al., 2008; Bozec et al., 2011; Stewart et al., 2017). However, gear deployments  
90 may induce avoidance or attraction behaviors that alter fish spatial distribution at scales larger  
91 than the sampled area which are not detectable without secondary sampling gear or an  
92 established calibration (Fréon et al., 1993; Yule et al., 2007; Schramm et al., 2020). For example,  
93 carnivorous individuals evenly distributed over a large reef area may contract their distribution  
94 around a baited camera rig but may expand their distribution to avoid a rapidly approaching  
95 mobile sampling gear.

96 Here, our objective was to assess behavioral responses to mobile video and acoustic  
97 sampling gears commonly used to survey reef fishes in the northern Gulf of Mexico (nGOM).  
98 Our model species was red snapper, *Lutjanus campechanus*, due to its abundance in the system,  
99 its ecological and economic importance in the region, and the fact that research efforts were  
100 being developed to produce an estimate of age-2+ abundance in US waters of the GOM. We  
101 estimated the behavioral response of red snapper to a mini ROV, a towed camera sled (TCS), a  
102 towed acoustic sled (TAS), and a diver (hereafter included when referring to mobile gears) at  
103 multiple scales. In the far field (up to 100 m from a reef), acoustic telemetry provided  
104 information on red snapper distance from reef, height off bottom, and acceleration to evaluate if  
105 fish were entering or exiting the surveyed area. Mid-field (up to 15 m from a reef) responses  
106 were examined with count data collected with a stationary, epibenthic horizontal-beam acoustic

107 profiler while near-field (up to 5 m from a reef) responses were examined with count and  
108 position data derived from stereo cameras positioned on the sea floor. Fish counts during mobile  
109 gear deployments were compared to counts during paired control periods prior to each gear  
110 deployment. Collecting data at these different spatial scales allowed us to produce a  
111 comprehensive assessment of whether red snapper displayed positive (attraction) or negative  
112 (avoidance) behaviors relative to mobile gears. Results have implications for surveys designed to  
113 estimate site-specific densities of red snapper or their absolute abundance in the Gulf of Mexico,  
114 as well as for assessing behavioral responses of other fish species to video or sonar sampling  
115 gears.

116

## 117 **2. Material and methods**

118

119 This study was conducted at a series of artificial reef sites (depth = 38-39 m) located  
120 approximately 35 nm SSE of Destin, Florida from September through November 2019 (Fig. 1A).  
121 Artificial reefs had been deployed by the Florida Fish and Wildlife Conservation Commission in  
122 2003 (Dance et al., 2011; Lewis et al., 2020) over featureless sand/mud bottom with a very  
123 gradual slope. Reefs were composed of 1 or 2 prefabricated concrete modules that were 1.83-3.1  
124 m tall with volumes of 4.1-4.9 m<sup>3</sup>. The coordinates of these reefs are not published, thus  
125 reducing the likelihood of fishery removals of tagged individuals during the study.

126

### 127 *2.1. Acoustic telemetry*

128

129 Proposed study reefs were first surveyed with the ROV in September 2019 to ensure red  
130 snapper aggregations were present prior to the deployment of the acoustic array. After  
131 identifying five reefs with sufficient red snapper abundance (>10 fish per site), an array of 70  
132 Vemco (Bedford, Nova Scotia, Canada) VR2Tx acoustic receivers was deployed on September  
133 25-26, 2019. Receivers were deployed 470 m apart in a 11.9 km<sup>2</sup> Vemco Positioning System  
134 (VPS) array such that all sampling reefs were located within the array and >500 m from the  
135 rectangular array perimeter (Fig. 1B). Receiver spacing and overall VPS array design was  
136 intended to provide high-resolution red snapper geolocation estimates and to maximize the  
137 probability of acoustic tag transmissions being detected by at least three receivers under  
138 predominant environmental conditions based on previous studies and range tests within this  
139 region (Dahl et al., 2020; Bohaboy et al., 2020). All acoustic receivers had internal  
140 synchronization transmitters set to 160 dB and were attached to the top of 2-m PVC support  
141 pipes with heavy duty UV stabilized nylon cable ties (250-lb tensile strength). An additional  
142 paracord safety line (550-lb tensile strength) was attached between each receiver and the 40-kg  
143 cement base (~0.5 m diameter) that anchored the PVC support pipe to the seafloor. A high-  
144 density foam buoy was attached to the top of the PVC pipe with a 2-m long section of paracord  
145 to enable the vessel captain to accurately identify the GPS coordinates of each receiver via the  
146 vessel's acoustic echo sounder (AIRMAR series) and chart plotter (Garmin GPSMAP series) for  
147 receiver recovery at the end of the experiment.

148 Red snapper (n = 50) were captured with hook-and-line at 5 study reefs (n = 10 fish per reef)  
149 within the acoustic array on October 28-29, 2019 and Vemco V9AP acoustic tags were  
150 externally attached following the methods of Bohaboy et al. (2020). Acoustic tags were  
151 programmed to emit a 151 dB unique acoustic identification code (ID) at 69 kHz with a 30

152 second mean transmission interval (range 15 to 45 sec) for 21 days. In addition to unique ID  
153 codes, acoustic tags also transmitted acceleration ( $m\cdot s^{-2}$ ) and depth converted pressure data (m),  
154 with the latter utilized to estimate depth occupied by tagged fish. Tags were attached externally  
155 using the method of Bohaboy et al. (2020) to minimize handling time, avoid surgery required for  
156 internal tagging, and facilitate quicker post-tagging acclimation. Following tagging, fish were  
157 attached to a descender device clamped onto their lower jaw, returned to depth, and released. The  
158 descender device was deployed with a small-diameter (~2.54 cm) handline rope and set to  
159 release fish at 4 atm (33 m). Two GoPro (Hero5) digital cameras in underwater housings were  
160 attached in line with the descender device to observe fish behavior (e.g., swimming activity and  
161 orientation) and potential depredation events during release of tagged fish (Bohaboy et al. 2020).  
162 The first camera was mounted 1 m above (oriented downward toward the seabed) and the second  
163 camera 1 m below (oriented upward toward the sea surface) the descender device.

164

## 165 *2.2. Red Snapper Behavioral Experiments*

166

167 Behavioral experiments were conducted on November 10 (sites 1 and 2), November 11  
168 (sites 3 and 4) and November 18 (sites 5) at study reefs where red snapper had been acoustically  
169 tagged and released at the end of October 2019. This provided at minimum a two-week  
170 acclimation period following tagging. This was determined to be adequate as 3D movement data  
171 indicated tag acclimation ( was accomplished after 2 days, which is consistent with findings  
172 reported by Bohaboy et al. (2020).

173 The sampling protocol, which began at least a half hour after sunrise and ended at least a  
174 half hour before sunset, was similar among all study reefs. Upon locating a given reef with the



175 ship's bottom profiler, a weighted aluminum camera stand was deployed to the seabed. The  
176 camera stand was equipped with four GoPro (Hero5) digital cameras housed in rigid waterproof  
177 cases. Stereo cameras were arranged in two pairs each with a baseline distance of 75 cm; the  
178 upper camera pair was mounted 15 cm above the bottom pair. The upper pair of stereo cameras  
179 was positioned 10° upward (oriented towards the surface) from horizontal while the lower pair  
180 were positioned parallel with the seafloor. All four cameras were positioned with a 10° toe-in  
181 angle and were set to 2.7k resolution at a frame rate of 60 fps. Cameras were fitted with  
182 extended-life batteries (24-hr maximum lifespan) to capture the entire experiment conducted at  
183 each reef with a single continuous video and single stereo camera system calibration. Prior to  
184 deployment at each reef site, a small flashlight was triggered in view of all four cameras  
185 immediately prior to deployment of the stand to allow for video synchronization and accurate  
186 stereo measurements during video analyses in the laboratory (Garner et al. 2021).

187 A benthic, stationary multibeam imaging sonar (500 kHz Mesotech M3) secured atop a 1-m  
188 tall tripod was deployed 15 m from each study reef to measure the broad-scale distribution of  
189 fish. The M3 was powered by an underwater battery system with an embedded computer to  
190 operate the sonar and record data. The M3 was angled horizontally to aim the major axis of the  
191 beam parallel and the minor axis perpendicular to the seabed. The M3 was configured to transmit  
192 a 120° (horizontal) by 30° (vertical) beam at 2 Hz, sampling out to a range of 25 m. In this  
193 configuration, the sampled beam volume was approximately 9,300 m<sup>3</sup>.

194 A 1-hour acclimation period followed deployment of the stereo-camera stand and M3, after  
195 which divers positioned the stereo-camera stand 5 m from the reef and the M3 15 m from the  
196 reef in their terminal position using a transect tape. The camera stand and M3 were positioned at  
197 90° headings relative to each other. GoPro Hero5 cameras have a vertical and horizontal field of

198 view of  $49.1^\circ$  and  $64.6^\circ$ , respectively, which results in a  $29.0 \text{ m}^2$  ( $4.6 \text{ m} \times 6.3 \text{ m}$ ) viewing  
199 window at a 5-m distance. Thus, the stereo cameras with a 75 cm baseline had a common  
200 viewing window of  $19.3 \text{ m}^2$  ( $4.6 \text{ m} \times 4.2 \text{ m}$ ) to track red snapper movements and collect length  
201 measurements. Stereo cameras were calibrated underwater by the diver positioning a  $5 \times 7$   
202 square ( $63.47 \text{ mm}$ ) checkerboard ( $610 \times 457 \text{ mm}$ ) at a variety of distances (between 1 and 5 m)  
203 and angles of incidence ( $<20^\circ$ ) following the methods of Delacy et al. (2017) and Garner et al.  
204 (2021). The diver began the calibration by positioning the checkerboard at 5 m distance (i.e.,  
205 adjacent to the reef) oriented towards the centerline of the camera stand and then swam slowly  
206 forward while tilting the checkerboard forwards, backwards, to the right, and to the left ( $20^\circ$   
207 range from perpendicular in each direction) in decreasingly large circular motions until the diver  
208 was 1 m from the camera stand (Delacey et al. 2017; Garner et al. 2021). The diver then repeated  
209 the same motions while swimming backwards and away from the camera stand towards the reef.  
210 The entire calibration procedure at each site required  $<5$  mins to complete. The circular  
211 checkerboard movements allowed the checkerboard to be viewed simultaneously by each camera  
212 pair during each transect while tilting the checkerboard increased contrast between paired images  
213 extracted in the laboratory during camera calibration.

214 Red snapper behavioral experiments commenced once the diver completed positioning the  
215 M3. Behavioral experiments at each reef site consisted of four 15-minute gear deployment  
216 periods and three 15-minute control periods (range: 14-21 min depending on haulback times)  
217 without mobile gears occurring in an alternating fashion (i.e., control, gear, control, gear etc).  
218 The diver treatment, which could not be randomized because it always preceded the other three  
219 survey gears, consisted of the 15-minute period immediately following positioning the stationary  
220 gears and the 15-minute control period immediately following the diver exiting the water. Each

221 of the three mobile survey gears (i.e., ROV, TCS, TAS) were then deployed in a randomized  
222 order with each preceded by a control period. Thus, the diver and the first mobile gear deployed  
223 at each site had a shared control period. The 15 min prior to diver deployment could not be used  
224 as the control period for the diver because the stereo cameras and M3 had not yet been  
225 positioned.

226 The ROV utilized in this study was a VideoRay Pro4 (375 x 289 x 223 mm; 6.1 kg; 305 m  
227 depth rating) equipped with an integrated live-view, forward-facing, internal camera (1080 p)  
228 and provided real-time depth and heading information. The TCS was a Towed Aquatic Resource  
229 Assessment System designed and built by Deep Ocean Engineering on a modified Phantom  
230 ROV frame and equipped with a Deep Sea Power & Light Multi SeaCam 2060 low-light color  
231 video camera, two 500 watt underwater lights (model 710-0400601), a Tritech PA200/20-PS  
232 sonar altimeter, a SeaLaser 100 parallel compass, and a depth (pressure) sensor. The TAS  
233 consisted of a 1 m by 0.25 m aluminum frame with 6.4 m thick PVC board “fins” attached for  
234 stability that carried a downward facing echosounder (70 kHz).

235 After positioning the stationary equipment, the diver proceeded to follow a mock point  
236 count method for a 15-min period (Bohnsack and Bannerot 1986; Patterson et al. 2009). During  
237 ROV deployments, it was flown as close to each reef as possible and flown in the immediate  
238 proximity (<10 m) of the reef for the duration of the 15-minute survey period following the same  
239 mock survey protocol as the diver. The TCS and TAS were each deployed approximately 100 m  
240 from each reef site and towed in three transects that crossed immediately above reefs such that  
241 each transect had a total distance of approximately 200 m. During TCS transects, the vessel  
242 maintained constant forward motion at intermittent speeds of 1-2 kts to maintain a target sled  
243 depth of 2-3 m above the seafloor. This was accomplished by monitoring the TCS’s integrated

244 depth sensor and live-feed camera in real time to ensure transects crossed over reefs. During  
245 TAS transects, the towing vessel maintained a speed of 3 kts and the sled remained at a depth of  
246 3 m below the sea surface. The stereo camera and M3 stands were retrieved by divers following  
247 the last mobile gear deployment at each site to extract digital video and sonar data. After all reef  
248 sites were sampled, acoustic telemetry receivers were retrieved from the seabed by divers  
249 between November 19 and 22, 2019.

250

### 251 *2.3. Data processing*

252

253 Data stored on acoustic receivers were downloaded onto a laptop in the field and the digital  
254 files were transmitted to Innovasea, Inc. in Dalhousie, Nova Scotia, Canada for post-processing  
255 with proprietary software (Espinoza et al. 2011; Smedbol et al. 2014). Geoposition (latitude and  
256 longitude coordinates), depth (m), and acceleration ( $m \cdot s^{-2}$ ) was estimated for each tag-specific  
257 acoustic ping heard by array receivers. Fate (e.g., tag loss, depredation, emigration) of  
258 acoustically tagged fish was estimated based on movement data following the approach of  
259 Bohaboy et al. (2020). Tags that were persistently stationary on the seafloor were assumed to  
260 have been shed. Tags that recorded acceleration values well above the mean for red snapper and  
261 with dramatic changes in geoposition were deemed predated if not viewed directly on video  
262 during the fish's return to depth with the descender device.

263 Video data were post-processed in the laboratory to estimate fish abundance and fork length  
264 (FL) to the nearest mm and track fish movements in response to mobile gear deployment. While  
265 the ROV, TCS, and TAS were the primary gear treatments of interest, diver presence was also  
266 included as a treatment in statistical analyses of video data because diver surveys are a

267 commonly used method to sample reef fish communities. During each 15-min gear deployment  
268 and the preceding 15-min control period, red snapper were counted from one camera of the top  
269 pair and one from the bottom pair. Camera-specific counts were estimated/annotated for each  
270 minute of each gear deployment and control period with counts defined as the maximum number  
271 of red snapper viewed during each minute of each 15-min period. Video or sonar data were not  
272 collected from any of the mobile gears or the diver; count data were taken only from the  
273 stationary camera stand and M3.

274 Red snapper tracking analysis performed on stereo camera video data utilized the freeware  
275 package XMAlab (Knörlein et al., 2016) available in R (R core team, 2019). X-ray motion  
276 analysis (XMA) software was developed to study *in vivo* skeletal movements in humans and  
277 animals using X-ray videos of surgically implanted radio-opaque markers but can also be applied  
278 to standard video files for tracking points identified on moving objects through a series of still  
279 images (Knörlein et al., 2016). Video data from stereo cameras were synchronized and stills of  
280 the checkerboard (n = 50) were extracted for calibration. Calibration files had <1% error for all  
281 but one reef site which had an estimation error of 1.5% due to a missing video segment that  
282 required manual synchronization prior to calibration. Each red snapper viewed simultaneously by  
283 both cameras of the stereo-camera pair was tracked if it remained in view for at least three  
284 seconds with a position estimated for each second the individual was in view. Tracking consisted  
285 of first identifying the anteriormost point of the jaw of an individual when first viewed by both  
286 cameras. Successive paired images were taken of that same individual every second (minimum  
287 of 3 seconds i.e., 3 still images) throughout the duration of its occurrence in the viewing window.  
288 Tracking concluded when the anteriormost point of the jaw exited the viewing window shared by  
289 both cameras or when it could no longer be confidently identified due to distance from the

290 camera (>5 m). Tracking data consisted of a set of x (left to right), y (top to bottom), and z (near  
291 to far) coordinates in real units (cm) with the origin point (0,0) corresponding to the center point  
292 of view shared by both cameras. The mean values for all initial and final positions (x, y, and z  
293 values) of all individuals tracked within each minute were estimated for each gear deployment  
294 treatment.

295       Following retrieval of the M3, acoustic data were downloaded and stored for analysis. Fish  
296 were detected and enumerated in Echoview (v10; Hobart, Australia) following methods  
297 described by Boswell et al. (2008). A background subtraction algorithm was applied to remove  
298 static background objects (i.e., substrate and reef structure), followed by a 3 x 3 median filter and  
299 multibeam single target detection algorithm. Targets that exceeded the minimum criteria (>30  
300 cm TL) were recorded for each ping (2 Hz), which thereby produces a time series of fish  
301 abundance (non-specific to species) associated with each site and used to compare with  
302 coincident estimates of counts from stereo-camera videos. Targets that met the minimum length  
303 criteria were enumerated in each ping and summed across each 1-minute interval so that  
304 abundance estimates could be compared with those derived from the cameras. To derive red  
305 snapper-specific abundance, the minute-specific count was then multiplied by the corresponding  
306 minute-specific proportion of red snapper observed on digital video. Video data indicated  
307 artificial reef study sites had low diversity (~5 species per site), and red snapper were the  
308 numerically dominant species at >30 cm TL, and other species were viewed infrequently. Thus,  
309 we were confident that partitioning echosounder fish abundance data using this method was  
310 robust.

311

312 *2.4. Statistical analyses*

313

314 A generalized linear model (GLM) was fit in R (R core team, 2019) to test the effect of FL  
315 and handling time on red snapper fate. Distance of red snapper from reef sites was estimated by  
316 calculating the distance between red snapper geolocation estimates and the center point of each  
317 reef site. We excluded geolocation estimates with horizontal position error (Smith, 2013) in the  
318 upper 5th percentile of the data to filter out estimates that were highly uncertain or likely resulted  
319 from false detections (Bohaboy et al., 2020). Geolocation estimates of red snapper >100 m from  
320 the study reef being examined were also excluded from statistical analysis of red snapper  
321 geolocation for the series of gear deployments at that reef. Depth data recorded on acoustic tags  
322 were converted to height off bottom (HOB; bottom depth – tag depth, m). Distance, HOB, and  
323 acceleration data were analyzed with separate generalized linear mixed models (GLMMs) with  
324 the “glmmTMB” package (Brooks et al., 2017) in R (R core team, 2019) with the general  
325 equation:

326

$$327 \quad Y = \beta_0 + \beta_1 X_1 + \beta_2 X_2 + \beta_3 X_1 X_2 + \nu + \omega + e, \quad Y \sim \text{Gamma}(\mu, \nu)$$

328

329 where  $Y$  is the response variable specified with a gamma distribution and link function specified  
330 as the log of the response value. Data values were  $\geq 0$  with a right skewed distribution and non-  
331 constant variance. The explanatory variables were gear presence ( $X_1$ ; deployment versus pre-  
332 deployment), time elapsed ( $X_2$ ; 1 to 15 min), and the interaction term. Fish ID and site were  
333 specified as random effects (intercepts) and are indicated by  $\nu$  and  $\omega$ , respectively. Model  
334 coefficients were exponentiated to allow interpretation on the original response scale. Separate

335 models were computed for each survey gear type (i.e., diver, ROV, TCS, or TAS). Residual  
336 diagnostic plots were utilized to examine model fit.

337 Red snapper count data derived from 1-min segments of M3 sonar and stereo-camera video  
338 were also analyzed with GLMMs but with the response variable for video samples being the  
339 mean number of red snapper observed per min, which was assumed to be Poisson-distributed  
340 with mean  $\lambda$ . For cameras, count data were computed as the average of the per-min counts  
341 between one top and bottom camera from each site. Separate GLMMs were estimated for each  
342 gear treatment where the mean red snapper count during the deployment period was compared to  
343 each gear's pre-deployment period. Minute also was included in each model as an explanatory  
344 variable along with the interaction term; site was included as a random effect. The AR1  
345 covariance structure was specified to account for autocorrelations among observations between  
346 time intervals but the option to specify zero-inflated data was not necessary. The same approach  
347 was used to analyze mean red snapper counts estimated with M3 sonar data, except that  
348 statistical models could not be estimated for the diver deployments due to interference from  
349 bubbles in the water column.

350

### 351 **3. Results**

352

353 Mean FL ( $\pm$  95%CI) of tagged red snapper was 448.1 mm ( $\pm$  27.4 mm) with individuals  
354 ranging from 325 to 620 mm. Thirty individuals were tagged at three study reefs on October 28,  
355 2019 and the remaining 20 were tagged at two sites on October 29, 2019 (Fig. 1B). Three of the  
356 initially tagged fish returned (floated) to the surface in poor condition and had their tags  
357 recovered and redeployed on different fish. Of the final 50 tagged individuals, 30 (60.0%)



358 survived and were detected at study reefs throughout the 22-day duration of the behavioral study,  
359 12 (24.0%) were likely depredated, 2 (3.3%) shed their tags, and 6 (12%) tags were never  
360 detected within the array. Results from GLM analysis indicated neither fish FL ( $p = 0.335$ ) nor  
361 handling time ( $p = 0.649$ ), or their interaction ( $p = 0.524$ ), significantly affected the probability  
362 of red snapper surviving and being detected throughout the study period.

363 There was a minimum of 4 and maximum of 7 acoustically tagged red snapper with unique  
364 ID tags present at each of the 5 survey reefs during gear deployments. In total, 1,004 geolocation  
365 estimates were logged during gear deployment periods among all red snapper behavioral  
366 experiments, which was 60.8% of acoustic pings emitted by tags during deployment periods.  
367 However, only 184 geolocation estimates occurred within 100 m reefs when mobile gears were  
368 actively deployed. Most of the remaining detections were due to individuals being detected at  
369 reef sites that were not actively being sampled. One tagged red snapper was estimated to be  
370 within 100 m of two different survey reef sites (sites 1 and 5) during gear deployments, but  
371 detections occurred 8 days apart.

372 Analysis of red snapper distance to reef, HOB, and acceleration data before and after the  
373 stereo camera and M3 sonar stands were deployed indicated no significant difference in red  
374 snapper distance to reef, HOB, or acceleration immediately after (post-deployment min 1-15)  
375 (Stands treatment), or well after (post-deployment min 16-60) deployment of the stereo camera  
376 and M3 sonar stands during the acclimation period (Acclimation) (Fig. 2; S Table 1). There was  
377 a significant effect of minute on red snapper acceleration ( $p = 0.007$ ) but the magnitude of the  
378 coefficient (1.02) was minimal. Analysis of red snapper counts per min during the acclimation  
379 period (i.e., prior to divers pointing the camera toward and 5 m from the reef) indicated fish

380 initially were seen in the view of the camera at elevated numbers that equilibrated to background  
381 levels after ~20-30 min during the acclimation period (Fig. 3).

382 Mean distance of tagged red snapper from study reefs during gear deployments was similar  
383 among diver, ROV, and TCS treatments and slightly lower during TAS deployments (Fig. 4A).  
384 Statistical models of mean red snapper distance to reefs during behavioral experiments indicated  
385 no significant gear effects existed (S Table 2). Red snapper HOB was less variable when the  
386 diver and ROV were deployed as compared to the other treatments but differed at most by only  
387 ~1 m among treatments (Fig, 4B). Height off bottom was not significantly different when the  
388 diver ( $p = 0.372$ ), ROV ( $p = 0.299$ ), or TAS ( $p = 0.458$ ) was present as compared to control  
389 periods, but the interaction between the TCS and minute was significant ( $p = 0.002$ ; S Table 3).  
390 Fish acceleration decreased during ROV and TAS gear deployments and increased during the  
391 diver deployments compared to control periods (Fig. 4C) but was not significantly different (S  
392 Table 4). Fish acceleration showed an overall decrease during TCS deployments (coefficient =  
393 0.26) but increased during the deployment period (TCS\*Minute term coefficient = 1.19;  $p$   
394 <0.001).

395 Analysis of stereo-camera video data indicated red snapper counts per minute were  
396 significantly greater during some gear deployments relative to their respective control periods (S  
397 Table 5; Fig. 5). The presence of the diver ( $p < 0.001$ ), ROV ( $p = 0.001$ ) or the TCS ( $p = 0.002$ )  
398 significantly affected mean red snapper counts. Mean per minute counts were 7.29 times higher  
399 during diver deployments, 1.89 times higher during ROV deployments, and 0.53 times lower  
400 during TCS deployments (S Table 5). The interaction term for TCS (TCS\*minute) was  
401 significant ( $p < 0.001$ ) indicating a positive increase in RS per minute during deployments. The  
402 TAS did not have a significant effect on RS mean counts per minute.

403 Red snapper counts estimated with the M3 sonar (Fig. 6) were similar to count estimates  
404 derived from video samples (Fig. 5) but results of statistical analyses differed. In contrast to  
405 models for near-field counts, statistical models for sonar-derived red snapper count estimates  
406 indicated no significant difference in counts per min for the ROV ( $p = 0.517$ ). Furthermore, the  
407 TCS had a significant positive overall effect on mean fish during deployment (coefficient = 3.34;  
408  $p < 0.001$ ) and a negative effect on mean fish per minute (coefficient of TCS\*Minute interaction  
409 = 0.88;  $p < 0.001$ ; S Table 6). The TAS had no significant effect on RS or counts per min and no  
410 significant interaction terms ( $p > 0.05$ ; S Tables 5 and 6). Visual inspection of mean red snapper  
411 counts per min derived from M3 sonar data show relatively stable mean ( $\pm$ SE) counts per min  
412 across all three gears except during mins 3 and 4 for the TCS where mean red snapper counts  
413 were 6.3 ( $\pm 4.2$ ) and 9.1 ( $\pm 7.4$ ), respectively (Fig. 6, column A). Inspection of scaled mean counts  
414 during these two time points well exceeded the overall mean of 2.4 ( $\pm 0.4$ ) fish per min for the  
415 TCS gear treatment (Fig. 6, column B).

416 Tracking data estimated for red snapper from stereo-camera video suggest behavioral  
417 responses in the near field in response to some survey gears. Overall, observed fish tended to be  
418 between 0.5 and 2 m above the seabed and within 3-4 m of reef modules. During TAS  
419 deployments, most red snapper were loosely aggregated above the reef with a few individuals in  
420 very close proximity (Fig 7D). During diver and ROV deployments, nearly all fish were  
421 aggregated above reefs, while fish were less tightly aggregated around the reef but nearer the  
422 seabed during TCS deployments (Fig. 7C).

423

#### 424 **4. Discussion**

425

426 Study results indicate that red snapper behavioral responses to the mobile survey gears  
427 examined in this study were observed in the near field at the smallest scale but not in the far field  
428 where fish would be considered entering or leaving the survey area. Therefore, we infer that  
429 none of the mobile survey gears examined would be likely to introduce substantial bias into  
430 estimates of red snapper because the number of red snapper associated with a reef site during a  
431 survey is constant. However, individuals just beyond the periphery of the area viewed during the  
432 survey could become identifiable and positively bias count data by approaching mobile gear.  
433 Video data reveal that red snapper can be inquisitive towards and approach foreign objects, like  
434 the stereo camera and M3 sonar stands, which might be interpreted as attraction when viewed  
435 only with gears that have small sampling volumes (10s of m<sup>3</sup>) that are much less than the  
436 volumes typically occupied by red snapper around reef sites (Piraino and Szedlmayer, 2014;  
437 Williams-Grove and Szedlmayer, 2016; Bohaboy et al., 2020). Generally, it is challenging to  
438 infer much about red snapper movement behavior from near-field video data alone because water  
439 clarity in the nGOM can be limited to <5 m at habitats closer to river outflows or after strong  
440 rain events, which makes it difficult to continuously track individuals seen on video (Stoner et  
441 al., 2008). High-resolution 3D acoustic telemetry provides critical movement information at  
442 spatial scales (100s of m) beyond the visual field of optical equipment and provides a robust  
443 evaluation on the potential for fish behavior to bias count data.

444 Response behavior by benthic fishes to survey gear (stationary or mobile) can be variable  
445 (Lorance and Trenkel, 2006; Stoner et al., 2008) and depend on light levels (Brock, 1982;  
446 Thorne et al., 1989; Ryer et al., 2009), habitat characteristics (Brock, 1982; Cailliet et al., 1999;  
447 Lawson and Rose, 1999; Edgar et al., 2004), gear characteristics (Koslow et al., 1999; Cailliet et  
448 al., 1999; Lorance and Trenkel, 2006; Stoner et al., 2008), and ecology (Norcross and Mueter,

449 1999; Lorange and Trenkel, 2006). In their synthesis of behavioral studies of fishes surveyed  
450 with underwater vehicles, Stoner et al. (2008) reported most of the taxa studied exhibited some  
451 type of response behavior to survey vehicles with more than half of the fish taxa examined  
452 exhibiting avoidance behavior while a third exhibited some degree of attraction. MacNeil et al.  
453 (2008) and Bozec et al. (2011) both reported that larger fishes on coral reefs tended to display  
454 stronger avoidance behavior. Somerton et al. (2017) observed near-field (10-20 m) negative  
455 response behaviors for vermilion snapper, *Rhomboplites aurorubens*, a congener commonly  
456 associated with red snapper at nGOM reefs, when approached by a TCS.

457       Despite being the most studied fishery species in the nGOM, little information exists in the  
458 published literature regarding responses of red snapper to fishery-independent mobile survey  
459 gears. We saw no evidence of avoidance behavior by red snapper in response to the presence of  
460 any of the survey gears used in this study. Startle responses were not observed on digital video  
461 and mean acceleration data were similar among nearly all gear treatments, as well as between  
462 paired gear deployment and control periods. Telemetry-derived geolocation data did not indicate  
463 an increase in mean distance from survey reefs, which would have been indicative of large-scale  
464 avoidance unobservable on video. Regardless, a negative behavioral response can only  
465 contribute to survey bias if the response directly or indirectly (e.g., startle response of individuals  
466 in view induces startle by others at the edge of or out of view) prevents species identification,  
467 increases enumeration error (e.g., blurring of individuals on video during startle response), or  
468 individuals avoid detection entirely. Although Stoner et al. (2008) caution against characterizing  
469 species-specific responses from a single study, we believe that red snapper are unlikely to  
470 demonstrate meaningful negative behavioral responses in subsequent studies because they can be  
471 inquisitive, are not cryptic, do not exhibit schooling behavior, are active with relatively low (0.5

472 m•sec<sup>-1</sup>) swimming speeds, and are readily distinguishable from other taxa and most congeners,  
473 thus allowing them to be confidently identified and enumerated.

474       Based on our video observations, gear attraction (positive bias) would be a more important  
475 potential issue than gear avoidance when conducting red snapper surveys, especially surveys  
476 designed to estimate absolute abundance. Although red snapper, especially small (<600 mm),  
477 young fish, are strongly reef-associated (Patterson et al., 2001; Westmeyer et al., 2007;  
478 Strelcheck et al., 2007; Bohaboy et al., 2020), they are a mobile species that may meander over  
479 areas 10s of m in radius from reef sites during daylight periods when collecting video data is  
480 feasible (Piraino and Szedlmayer, 2014; Williams-Grove and Szedlmayer, 2016; Bohaboy et al.,  
481 2020). Therefore, there is considerable potential for red snapper to contract the volume they  
482 occupy around reefs during surveys if they respond positively to survey gear. Such a contraction  
483 of their distribution could arise through inquisitive actions towards the gear or through a flight  
484 response that concentrates them nearer to reef structure. Despite this potential for positive bias,  
485 neither telemetry data nor benthic sonar indicated any large- or medium-scale attraction of red  
486 snapper to the initial stereo camera or M3 stand deployments or during deployment of the survey  
487 gears. Fish did display positive bias at the smallest-scale ( $\leq 5$  m) when the diver or ROV were  
488 deployed, presumably due to LEDs associated with the ROV's electronics, general curiosity, or  
489 disturbance of potential benthic food items by the diver's fins. However, when the different data  
490 sources are examined together, the potential for bias is likely to be relatively small because it  
491 was only observed at the smallest scale and only affected by individuals near the periphery of the  
492 viewed area.

493       Red snapper behavioral responses were more complex for the TCS given a potential  
494 attraction issue was observed during the TCS deployment at reef site 1. Several red snapper were

495 seen oriented toward but swimming behind (i.e., following behavior) the TCS on two of three  
496 transects when it passed over the reef in view of the benthic cameras. However, we did not detect  
497 directional movements or red snapper following behavior when the TCS was deployed at the  
498 other four reef sites. The individuals observed following the TCS at site 1 also were unlikely to  
499 meaningfully bias survey-derived density estimates because they were initially observed to  
500 exhibit typical swimming behavior and only began orienting towards the TCS as it passed the  
501 reef module. During the period they exhibited following behavior, these fish had already been  
502 viewed by the TCS's forward-facing camera and were out of view when they began following  
503 the sled. A towed camera sled deployed in a single unidirectional transect over relatively great  
504 distances with forward-facing cameras would not record following behavior and thus avoid that  
505 source of numerical bias when estimating animal density for the area surveyed. However,  
506 individuals near the periphery approaching the gear would have a similar effect on counts as  
507 during diver or ROV deployments. Geoposition estimates of acoustically tagged red snapper  
508 indicated following behavior was over very short distances as we did not observe an increase in  
509 distance from the reef during TCS surveys nor an increase in the variance associated with the  
510 distance of tagged red snapper from the reef compared to other treatments.

511 Red snapper swimming behavior was not affected by the TAS at any scale. Issues with  
512 survey bias have been previously reported with TAS-type gear when surveying demersal fishes  
513 associated with complex habitats if the fishes seek vertical or structural refuge in response to  
514 hydrodynamic (i.e., pressure waves) or auditory (i.e., vessel noise) stimuli (Lawson and Rose,  
515 1999; Kotwicki et al., 2013; Kotwicki et al., 2015). Potential detectability issues are well-known  
516 with TAS gears in complex benthic habitats, especially ones with vertical relief, due to acoustic  
517 shadows or "dead zones" that reduce fish detectability (Ona and Mitsen, 1996; Hjellvik et al.,

518 2003; Kotwicki et al., 2013). In this study, the TAS was deployed approximately 3 m below the  
519 surface at reef sites that were nearly 40 m deep, thus minimizing the possibility of red snapper  
520 displaying behavioral reactions to the TAS. No vertical response behaviors (e.g., synchronized  
521 downward directional swimming or persistent changes in proximity to the benthic surface) by  
522 red snapper were observed on stereo-camera video during TAS tows. Stereo-camera tracking  
523 data also indicated red snapper were the most dispersed around reefs during TAS deployments,  
524 and 3D telemetry data indicated no effect of the TAS on red snapper position or movement  
525 metrics.

526 Red snapper counts were higher when the stereo camera and M3 sonar stands were first  
527 deployed, but that effect dissipated over a relatively short time period (10s of min). The stands  
528 were the first gear introduced at each of the survey sites and they disturbed the sediment when  
529 they landed on the seabed, which may have explained the initial attraction of red snapper if the  
530 fish perceived the disturbed or suspended sediment as a feeding opportunity. Divers working on  
531 the seabed to move the stereo camera and M3 sonar stands into position also disturbed the  
532 sediment and thus possibly exposed benthic prey fauna. This could explain the persistent rather  
533 than fleeting attraction of fish to the divers as well as the greater magnitude of the effect  
534 compared to the ROV.

535 Overall, study results indicate that none of the survey gears used in this study were likely to  
536 elicit a strong behavioral response that would substantially bias count estimates at relevant  
537 spatio-temporal scales. However, there are two caveats to this interpretation. First, stereo camera  
538 and M3 sonar stands always were deployed first at each reef site in our multidisciplinary attempt  
539 to estimate the effect of mobile survey gears on red snapper behavior. It is unknowable from our  
540 design whether red snapper would have displayed different behavior in response to any one of



541 the mobile survey gears if it had been the first or only gear deployed at a reef. Field surveys  
542 typically consist of only one survey gear type per sample site. Although future studies could test  
543 potential attraction issues with only a single response measurement method per site (i.e.,  
544 telemetry, acoustic sonar, or stereo cameras), which in hindsight perhaps should have been done  
545 at additional study reefs, it was important to measure the behavioral response at multiple scales.

546 A second caveat to interpreting study results with respect to mobile survey gear effects on  
547 red snapper swimming behavior is that all experimental work was performed at artificial reefs  
548 that were distributed on otherwise featureless sand bottom. The reason for conducting the  
549 experiment in this habitat was because the probability of locating red snapper on nGOM artificial  
550 reefs is much higher than on natural reefs (Dance et al., 2011; Patterson et al., 2014) where their  
551 density is typically an order of magnitude lower for reefs on the nGOM shelf (Patterson et al.,  
552 2014; Karnauskas et al., 2017). There are no published studies on red snapper swimming or  
553 foraging behavior on natural reefs, thus no comparisons with results from the numerous  
554 published red snapper acoustic telemetry papers is possible. If artificial reefs altered red snapper  
555 movement behavior, then study results may not provide an accurate picture of how the mobile  
556 survey gears examined affect red snapper behavior, or whether patterns observed are likely to be  
557 applicable to natural reef habitats as well. However, red snapper are known to move >50 m away  
558 from artificial reefs (Piraino and Szedlmayer, 2014; Bohaboy et al., 2020), which was seen in the  
559 current study as well, thus are not closely site-attached to the structure of artificial reefs.  
560 Furthermore, adult red snapper trophic position and diet, which ranges from small zooplankton  
561 to relatively large fishes, are consistent between natural and artificial reefs (Tarnecki and  
562 Patterson, 2015), thus indicating red snapper foraging behavior directed at mostly non-reef prey  
563 is consistent between the habitat types.

564 In conclusion, results from this study indicate that the mobile survey gears typically used to  
565 collect density estimates at scales necessary for population assessment (i.e., ROV, TCS, or TAS)  
566 had minimal effects on mid or far field red snapper behavior. Therefore, we found minimal  
567 evidence for the major potential source of error: large-scale movements away from or towards  
568 survey reefs that would significantly bias red snapper abundance or density estimates. Small-  
569 scale movements within the area surveyed could positively bias count estimates made with  
570 mobile gears operating near reef structure or the seafloor, but this would likely involve few fish  
571 relative to the viewed area (i.e., only fish near the periphery of view). Fishery-independent  
572 surveys utilizing a variety of gears have become an integral part of stock assessments, but  
573 abundance data are also important for examining ecological questions, including via ecosystem  
574 models. This study was not designed to compare red snapper abundance or density estimates  
575 among the gears examined to develop gear-specific correction factors, but the issue of  
576 detectability is important depending on whether optical or sonar approaches are utilized in a  
577 given survey. Quantifying potential gear biases can help reduce variability in density estimates or  
578 indices of abundance and thus reduce scientific uncertainty in stock assessments or reduce  
579 measurement error in ecosystem models. Understanding the sources and magnitude of gear bias  
580 can also increase stakeholder confidence and acceptance of management regulations that in turn  
581 can help achieve management objectives.

582

583

584 **Acknowledgements**

585

586 Funding for this work was provided by a grant from Sea Grant and the National Marine  
587 Fisheries Service (#NA16OAR4170181) and the Florida Fish and Wildlife Research Institute  
588 (#FWC-16188) to WFP. We greatly appreciate the efforts of Erin Bohaboy in providing  
589 technical details and guidance for acoustic tagging methodology and data processing. We thank  
590 Jessica VanVaerenbergh and Savannah Lebuja for field support during field experiments. We  
591 also gratefully acknowledge the captain and crew of the charterboat vessel Dreadknot II for the  
592 invaluable assistance they provided in the field.

593 **References**

594

595 Bohaboy, E.C., Guttridge, T.L., Hamerschlag, N., Van Zinnicq Bergmann, M.P., Patterson III, W.F., 2020.

596 Application of three-dimensional acoustic telemetry to assess the effects of rapid recompression on reef fish  
597 discard mortality. *ICES J. Mar. Sci.* 77, 83-96. <https://doi.org/10.1093/icesjms/fsz202>.

598 Bohnsack, J.A., Bannerot, S.P., 1986. A stationary visual census technique for quantitatively assessing community  
599 structure of coral reef fishes. NOAA Tech. Rep. No. 41, 21 pp.

600 Boswell, K.M., Wilson, M.P., Cowan Jr, J.H., 2008. A semiautomated approach to estimating fish size, abundance,  
601 and behavior from dual-frequency identification sonar (DIDSON) data. *N. Am. J. Fish. Manage.* 28, 799-  
602 807. <https://doi.org/10.1577/M07-116.1>.

603 Bozec, Y.-M., Kulbicki, M., Laloe, F., Mou-Tham, G., Gascuel, D., 2011. Factors affecting the detection distances  
604 of reef fish: implications for visual counts. *Mar. Biol.* 158, 969-981. [https://doi.org/10.1007/s00227-011-](https://doi.org/10.1007/s00227-011-1623-9)  
605 1623-9.

606 Brock, R.E., 1982. A critique of the visual census method for assessing coral reef fish populations. *Bull. Mar. Sci.*  
607 32, 269-276.

608 Brooks, M.E., Kristensen, K., van Benthem, K.J., Magnusson, A., Berg, C.W., Nielsen, A., Skaug, H.J., Maechler,  
609 M., Bolker, B.M., 2017. glmmTMB balances speed and flexibility among packages for zero-inflated  
610 generalized linear mixed modeling. *R J.* 9, 378-400. <https://doi.org/10.3929/ethz-b-000240890>.

611 Cailliet, G.M., Andrews, A.H., Wakefield, W.W., Moreno, G., Rhodes, K.L., 1999. Fish faunal and habitat analyses  
612 using trawls, camera sleds, and submersibles in the benthic deep-sea habitats off central California.  
613 *Oceanologica Acta* 22, 579-592.

614 Chen, Y., Chen, L., Stergiou, K.I., 2003. Impacts of data quantity on fisheries stock assessment. *Aquat. Sci.* 65, 1-  
615 07. <https://doi.org/10.1015-1621/03/010001-07>.

616 Dahl, K.A., Patterson III, W.F., 2020. Movement, home range, and depredation of adult invasive lionfish revealed  
617 by fine-scale acoustic telemetry in the northern Gulf of Mexico. *Mar. Biol.* 167, 1-22.  
618 <https://doi.org/10.1007/s00227-020-03728-4>.

619 Davison, P.C., Koslow, J.A., Kloser, R.J., 2015. Acoustic biomass estimation of mesopelagic fish: backscattering  
620 from individuals, populations, and communities. *ICES J. Mar. Sci.* 72, 1413-1424.  
621 <https://doi.org/10.1093/icesjms/fsv023>.

622 Delacy, C.R., Olsen, A., Howey, L.A., Chapman, D.D., Brooks, E.J., Bond, M.E., 2017. Affordable and accurate  
623 stereo-video system for measuring dimensions underwater: a case study using oceanic whitetip sharks  
624 *Carcharhinus longimanus*. *Mar. Ecol. Prog. Ser.* 574, 75-84. <https://doi.org/10.3354/meps12190>.

625 Dickens, L.C., Goatley, C.H.R., Tanner, J.K., Bellwood, D.R., 2011. Quantifying relative diver effects in  
626 underwater visual censuses. *PLOS ONE.* 6(4), e18965. <https://doi.org/10.1371/journal.pone.0018965>.

627 Edgar, G.J., Barrett, N.S., Morton, A.J., 2004. Biases associated with the use of underwater visual census techniques  
628 to quantify the density and size-structure of fish populations. *J. Exp. Mar. Biol. Ecol.* 308, 269-290.  
629 <https://doi.org/10.1016/j.jembe/2004.03.004>.

630 Edgar, G.J., Stuart-Smith, R.D., 2014. Systematic global assessment of reef fish communities by the Reef Life  
631 Survey program. *Sci. Dat.* 1, 1-8. <https://doi.org/10.1038/sdata.2014.7>.

632 Espinoza, M., Farrugia, T.J., Webber, D.M., Smith, F., Lowe, C.G., 2011. Testing a new acoustic telemetry  
633 technique to quantify long-term, fine-scale movements of aquatic animals. *Fish. Res.* 108, 364–371.  
634 <https://doi.org/10.1016/j.fishres.2011.01.011>.

635 FAO (Food and Aquaculture Organization), 2018. *The state of world fisheries and aquaculture*. Rome. 227 pp.

636 Fauconnet, L., Rochet, M.-J., 2016. Fishing selectivity as an instrument to reach management objectives in an  
637 ecosystem approach to fisheries. *Mar. Pol.* 64, 46-54. <https://doi.org/10.1016/j.mar.pol.2015.11.004>.

638 Fréon, P., Gerlotto, F., Misund, O.A., 1993. Consequences of fish behavior for stock assessment. *ICES Mar. Sci.*  
639 *Sym.* 196, 190-195.

640 Garner, S.B., Olsen, A.M., Caillouet, R., Campbell, M.D., Patterson III, W.F. 2021. Estimating reef fish size  
641 distributions with a mini remotely operated vehicle-integrated stereo camera system. *PLOS ONE.* 16,  
642 e0247985. <https://doi.org/10.1371/journal.pone.0247985>.

643 Haddon, M., 2010. *Modelling and quantitative methods in fisheries*. CRC press.

644 Hamilton, S.L., Caselle, J.E., Standish, J.D., Schroeder, D.M., Love, M.S., Rosales-Casian, J.A., Sosa-Nishizaki, O.  
645 2007. Size-selective harvesting alters life histories of a temperate sex-changing fish. *Ecol. Appl.* 17, 2268-  
646 280. <https://doi.org/10.1890/06-1930.1>.

647 Harvey, E.S., Cappel, M., Butler, J.J., Hall, N., Kendrick, G.A., 2007. Bait attraction affects the performance of  
648 remote underwater video stations in assessment of demersal fish community structure. *Mar. Ecol. Prog. Ser.*  
649 350, 245-254. <https://doi.org/10.3354/meps07192>.

650 Hjellvik, V., Michalsen, K., Aglen, A., Nakken, O., 2003. An attempt at estimating the effective fishing height of the  
651 bottom trawl using acoustic survey recordings. *ICES J. Mar. Sci.* 60, 967-979. [https://doi.org/10.1016/S1054-3139\(03\)00116-4](https://doi.org/10.1016/S1054-3139(03)00116-4).

652

653 Hutchings, J.A., Minto, C., Ricard, D., Baum, J.K., Jensen, O.P., 2010. Trends in the abundance of marine fishes.  
654 *Can. J. Fish. Aquat. Sci.* 67, 1205-1210. <https://doi.org/10.1139/F10-081>.

655 Keiter, D.A., Davis, A.J., Rhodes, O.E., Cunningham, F.L., Kilgo, J.C., Pepin, K.M., Beasley, J.C., 2017. Effects of  
656 scale of movement, detection probability, and true population density on common methods of estimating  
657 population density. *Sci. Rep.* 7, 1-12. <https://doi.org/10.1038/s41598-017-09746-5>.

658 Knörlein, B.J., Baier, D.B., Gatesy, S.M., Laurence-Chasen, J.D., Brainerd, E.L., 2016. Validation of XMA Lab  
659 software for marker-based XROMM. *J. Exp. Biol.* 219, 3701-3711. <https://doi.org/10.1242/jeb.145383>.

660 Koslow, J.A., Kloser, R., Stanley, C.A., 1995. Avoidance of a camera system by a deepwater fish, the orange roughy  
661 (*Hoplostethus atlanticus*). *Deep-Sea Res. Pt I.* 42, 233-244.

662 Kotwicki, S., Robertis, A.D., Ianelli, J.N., Punt, A.E., Horne, J.K., 2013. Combining bottom trawl and acoustic data  
663 to model acoustic dead zone correction and bottom trawl efficiency parameters for semipelagic species. *Can.*  
664 *J. Fish. Aquat. Sci.* 70, 208-219. <https://doi.org/10.1139/cjfas-2012-0321>.

665 Kotwicki, S., Horne, J.K., Punt, A.E., Ianelli, J.N., 2015. Factors affecting the availability of walleye pollock to

666 acoustic and bottom trawl survey gear. ICES J. Mar. Sci. 72, 1425-1439.  
667 <https://doi.org/10.1093/icesjms/fsv011>.

668 Langlois, T.J., Harvey, E.S., Fitzpatrick, B., Meeuwig, J.J., Shedrawi, G., Watson, D.L., 2010. Cost-efficient  
669 sampling of fish assemblages: comparison of baited video stations and diver video transects. Aquat. Biol. 9,  
670 155-168. <https://doi.org/10.3354/ab00235>.

671 Lawson, G.L., Rose, G.A., 1999. The importance of detectability to acoustic surveys of semi-demersal fish. ICES J.  
672 Mar. Sci. 56, 370-380.

673 Letessier, T.B., Juhel, J.-B., Vigliola, L., Meeuwig, J.J., 2015. Low-cost small action cameras in stereo generates  
674 accurate underwater measurements of fish. J. Exp. Mar. Biol. Ecol. 466, 120-126.  
675 <https://doi.org/10.1016/j.jembe.2015.02.013>.

676 Lorance, P., Trenkel, V.M., 2006. Variability in natural behavior, and observed reactions to an ROV, by mid-slope  
677 fish species. J. Exp. Mar. Biol. Ecol. 332, 106-119. <https://doi.org/10.1016/j.jembe.2005.11.007>.

678 MacNeil, M.A., Tyler, E.H.M., Fonnesebeck, C.J., Rushton, S.P., Polunin, N.V.C., Conroy, M.J., 2008. Accounting  
679 for detectability in reef-fish biodiversity estimates. Mar. Ecol. Prog. Ser. 367, 249-260.  
680 <https://doi.org/10.3354/meps07580>.

681 Marques, T.A., Thomas, L., Martin, S.W., Mellinger, D.K., Ward, J.A., Moretti, D.J., Harris, D., Tyack, P.L., 2013.  
682 Estimating animal population density using passive acoustics. Biol. Rev. 88, 287-309.  
683 <https://doi.org/10.1111/brv.12001>.

684 Maunder, M.N., Punt, A.E., 2013. A review of integrated analysis in fisheries stock assessment. Fish. Res. 142, 61-  
685 74. <https://doi.org/10.1016/j.fishres.2012.07.025>.

686 Norcross, B.L., Mueter, F.-J., 1999. The use of an ROV in the study of juvenile flatfish. Fish. Res. 39, 241-251.

687 Patterson, W.F., Cowan Jr., J.H., Wilson, C.A., Shipp, R.L., 2001. Age and growth of red snapper, *Lutjanus*  
688 *campechanus*, from an artificial reef area of Alabama in the northern Gulf of Mexico. Fish. Bull. 99, 617-  
689 627.

690 Patterson, W.F., Tarnecki, J.H., Addis, D.T., Barbieri, L.R., 2014. Reef fish community structure at natural versus  
691 artificial reefs in the northern Gulf of Mexico. GCFI. 66, 4-8.

692 Piraino, M.N., Szedlmayer, S.T., 2014. Fine-scale movements and home ranges around artificial reefs in the  
693 northern Gulf of Mexico. T. Am. Fish. Soc. 143, 988-998. <https://doi.org/10.1080/00028487.2014.901249>.

694 R Core Team, 2019. R: A language and environment for statistical computing. R Foundation for Statistical  
695 Computing. Vienna, Austria.

696 Ramsey, D.S., Caley, P.A., Robley, A., 2015. Estimating population density from presence-absence data using a  
697 spatially explicit model. J. Wildlife. Manage. 79, 491-499. <https://doi.org/10.1002/jwmg.851>.

698 Rivoirard, J., Simmonds, J., Foote, K.G., Fernandes, P., Bez, N., 2008. Geostatistics for estimating fish abundance.  
699 John Wiley & Sons.

700 Ryer, C.H., Stoner, A.W., Iseri, P.J., Spencer, M.L., 2009. Effects of simulated underwater vehicle lighting on fish  
701 behavior. Mar. Ecol. Prog. Ser. 391, 97-106. <https://doi.org/10.3354/meps08168>.

702 Schramm, K.D., Harvey, E.S., Goetze, J.S., Travers, M.J., Warnock, B., Saunders, B.J., 2020. A comparison of

703 stereo-BRUV, diver operated and remote stereo-video transects for assessing reef fish assemblages. *J. Exp.*  
704 *Mar. Biol. Ecol.* 524, 151273. <https://doi.org/10.1016/j.jembe.2019.151273>.

705 Smedbol, S.J., Smith, F., Weber, D.M., Vallee, R.E., King, T.D., 2014. Using underwater coded acoustic telemetry  
706 for fine scale positioning of aquatic animals. 20th Symposium of the International Society on Biotelemetry  
707 Proceedings. pp. 9-11.

708 Somerton, D.A., Gledhill, C.T., 2005. Report on the National Marine Fisheries Service workshop on underwater  
709 video analysis. NOAA Tech. Memo. NMFS-F/SPO-68.

710 Somerton, D.A., Williams, K., Campbell, M.D., 2017. Quantifying the behavior of fish in response to a moving  
711 camera vehicle by using benthic stereo cameras and target tracking. *Fish. Bull.* 115, 343-354.  
712 <https://doi.org/10.7755/FB.115.3.5>.

713 Stewart, D.R., Butler, M.J., Harris, G., Johnson, L.A., Radke, W.R., 2017. Estimating abundance of endangered fish  
714 by eliminating bias from non-constant detectability. *Endanger. Species Res.* 32, 187-201.  
715 <https://doi.org/10.3354/esr00792>.

716 Stoner, A.W., Ryer, C.H., Parker, S.J., Auster, P.J., Wakefield, W.W., 2008. Evaluating the role of fish behavior in  
717 surveys conducted with underwater vehicles. *Can. J. Fish. Aquat. Sci.* 65, 1230-1243.  
718 <https://doi.org/10.1139/F08-032>.

719 Strelcheck, A.J., Cowan Jr., J.H., Patterson III, W.F., 2007. Site fidelity, movement, and growth of red snapper:  
720 implications for artificial reef management. In: Patterson III, W.F., Cowan Jr, J.H., Fitzhugh, G.R., Nieland,  
721 D.L. (eds.), *Red snapper ecology and fisheries in the U.S. Gulf of Mexico*. AFS Sym. 60, 147-162.

722 Stuart-Smith, R.D., Bates, A.E., Lefcheck, J.S., Duffy, J.E., Baker, S.C., Thompson, R.J., Stuart-Smith, J.F., Hill,  
723 N.A., Kininmonth, S.J., Airoidi, L., Becerro, M.A., Campbell, S.J., Dawson, T.P., Navarrete, S.A., Soler,  
724 G.A., train, E.M.A., Willis, T.J., Edgar, G.J., 2013. Integrating abundance and functional traits reveals new  
725 global hotspots of fish diversity. *Nature*. 501, 539-542. <https://doi.org/10.1038/nature/12529>.

726 Tarnecki, J.H., Patterson III, W.F., 2015. Changes in red snapper diet and trophic ecology following the Deepwater  
727 Horizon oil spill. *Mar. Coast. Fish.* 7, 135-147. <https://doi.org/10.1080/19425120.2015.1020402>.

728 Thompson, A.A., Mapstone, B.D., 1997. Observer effects and training in underwater visual surveys of reef fishes.  
729 *Mar. Ecol. Prog. Ser.* 154, 53-63.

730 Thorne, R.E., Hedgepeth, J.B., Campos, J., 1989. Hydroacoustic observations of fish abundance and behavior  
731 around an artificial reef in Costa Rica. *Bull. Mar. Sci.* 44, 1058-1064.

732 Westmeyer, M.P., Wilson III, C.A., Nieland, D.L., 2007. Fidelity of red snapper to petroleum platforms in the  
733 northern Gulf of Mexico. In: Patterson III, W.F., Cowan Jr, J.H., Fitzhugh, G.R., Nieland, D.L. (eds.), *Red*  
734 *snapper ecology and fisheries in the U.S. Gulf of Mexico*. AFS Sym. 60, 105-121.

735 Williams-Grove L.J., Szedlmayer, S.T., 2016. Acoustic positioning and movement patterns of red snapper *Lutjanus*  
736 *campechanus* around artificial reefs in the northern Gulf of Mexico. *Mar. Ecol. Prog. Ser.* 53, 233-251.  
737 <https://doi.org/10.3354/meps11778>.

738 Yule D.L., Adams, J.V., Stockwell, J.D., Gorman, O.T., 2007. Using multiple gears to assess acoustic detectability

739 and biomass of fish species in Lake Superior. *N. Am. J. Fish. Manage.* 27, 106-126.  
740 <https://doi.org/10.1577/M06-090.1>.  
741 Zenone A.M., Burkepile, D.E., Boswell, K.M., 2017. A comparison of diver vs. acoustic methodologies for  
742 surveying fishes in a shallow water coral reef ecosystem. *Fish. Res.* 189, 62-66.  
743 <https://doi.org/10.1016/j.fishres.201701.007>.



## FIGURE LIST

**Fig. 1.** Location of array (red dot inside red box) in A) the central northern Gulf of Mexico ~35 nm southeast of Destin, FL, and B) locations of reef sites within the 4.23 x 2.82 km (11.9 km<sup>2</sup>) acoustic array. Numbered circles indicate acoustic receiver positions while triangles indicate artificial reef sites. Numbered triangles indicate site locations where, and the order in which, red snapper were tagged with acoustic transmitters and released (10 per site). No fish were tagged at reef sites indicated by numberless triangles. Receivers were deployed 472 m apart in any cardinal direction all with equal spacing.

**Fig. 2.** Distance to reef (m), height off bottom (m), and acceleration (m•s<sup>2</sup>) of acoustically tagged red snapper at survey reefs 55 minutes prior to and after the stereo camera and M3 sonar stands were deployed. Individual data points are means ± 95% CIs of 5-min time bins. The vertical gray line indicates timing of stand deployment.

**Fig. 3.** Exponential decline of red snapper observed on digital video during the initial acclimation period at each site, prior to divers being deployed to position the stereo camera and M3 sonar stands. The acclimation period began when the stereo camera stand contacted the seabed and ended when the diver entered the water to position the stands. Data plotted are mean ±SE red snapper counts per minute at the 5 sites surveyed. The fitted line is a non-linear regression with its equation indicated on the figure.

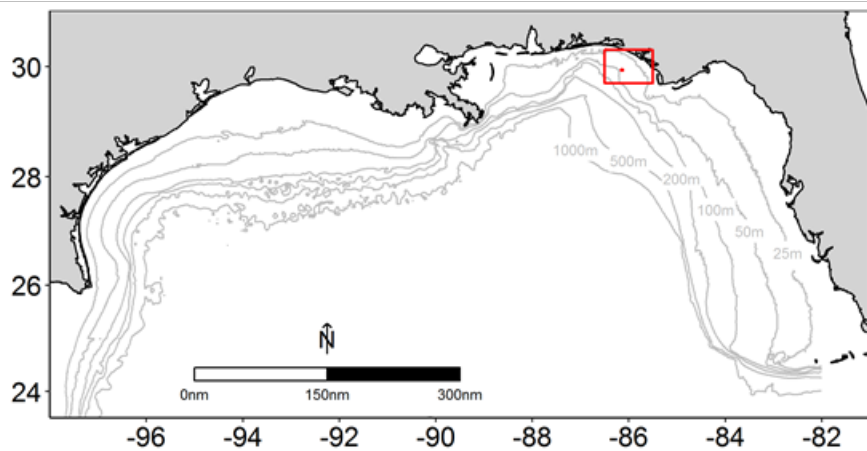
**Fig. 4.** Plots of A) mean distance (m), B) depth (m), or C) acceleration (m•s<sup>2</sup>) of acoustically tagged red snapper that were near the survey site (≤100 m) where the diver, remotely operated vehicle (ROV), towed camera sled (TCS), or towed acoustic sled (TAS) were actively deployed (filled circles) as well as during their respective control periods (filled triangles). Sample sizes are shown above each point. Error bars indicate ±SE.

**Fig. 5.** Mean (column A) and scaled mean (column B) counts of red snapper observed per minute on digital video during the diver (dark gray), remotely operated vehicle (gold), towed camera sled (dark blue), or towed acoustic sled (dark orange) gear treatments. Scaled mean values were

estimated by subtracting the site-specific mean for the 15-minute period before each gear deployment from the mean count estimate per minute for each gear treatment. Mean values shown at the top right of each panel in the left column indicate the overall mean of the pre-deployment period for each gear treatment. Error bars indicate  $\pm$ SE.

**Fig. 6.** Mean (column A) and scaled mean (column B) counts of red snapper observed per minute with a lateral-viewing, benthic echosounder (M3) during the remotely operated vehicle (gold), towed camera sled (dark blue), or towed acoustic sled (dark orange) gear treatments. Scaled mean values were estimated by subtracting the site-specific mean (shown on panels in column A) for the 15-minute period before each gear deployment from the mean count estimate per minute for each gear treatment. Mean values shown at the top right of each panel in the left column indicate the overall mean of the pre-deployment period for each gear treatment. Error bars indicate  $\pm$ SE. The diver treatment could not be included due to acoustic interference.

**Fig. 7.** Minute-specific mean directional red snapper movement computed from stereo camera tracking of individual fish during the A) diver, B) remotely operated vehicle, C) towed camera sled, or D) towed acoustic sled gear deployments among all study sites. The black triangle indicates the position of the artificial reef module relative to the stereo camera stand (black square) oriented towards the reef. The number of observations contributing to each mean position is indicated by the number at each arrowhead, while the legend indicates the observed minute during the 15-min gear deployment.

**A****B**